Intelligent Vehicle Safety Systems

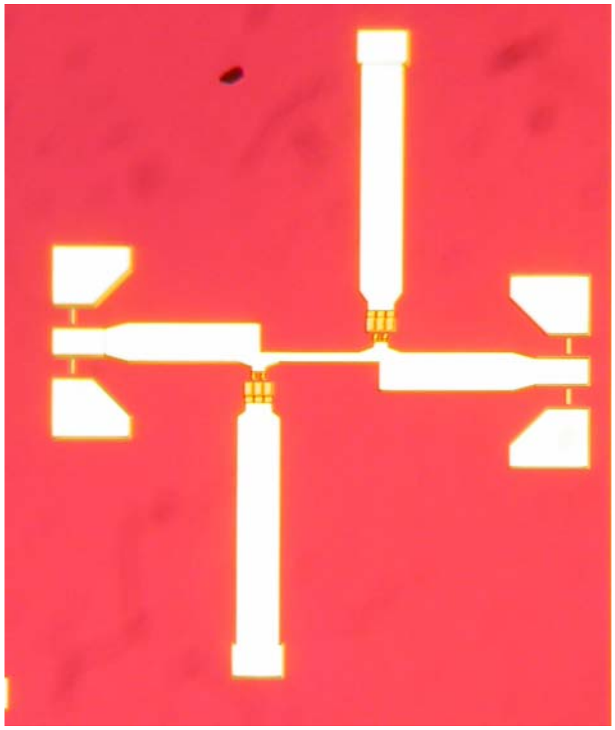

A low-cost electrically steerable active antenna for adaptive cruise control and other applications

IVSS Project Report

The IVSS Programme

The IVSS programme was set up to stimulate research and development for the road safety of the future. The result will probably be new, smart technologies and new IT systems that will help reduce the number of traffic-related fatalities and serious injuries.

IVSS projects shall meet the following three criteria: road safety, economic growth and commercially marketable technical systems.

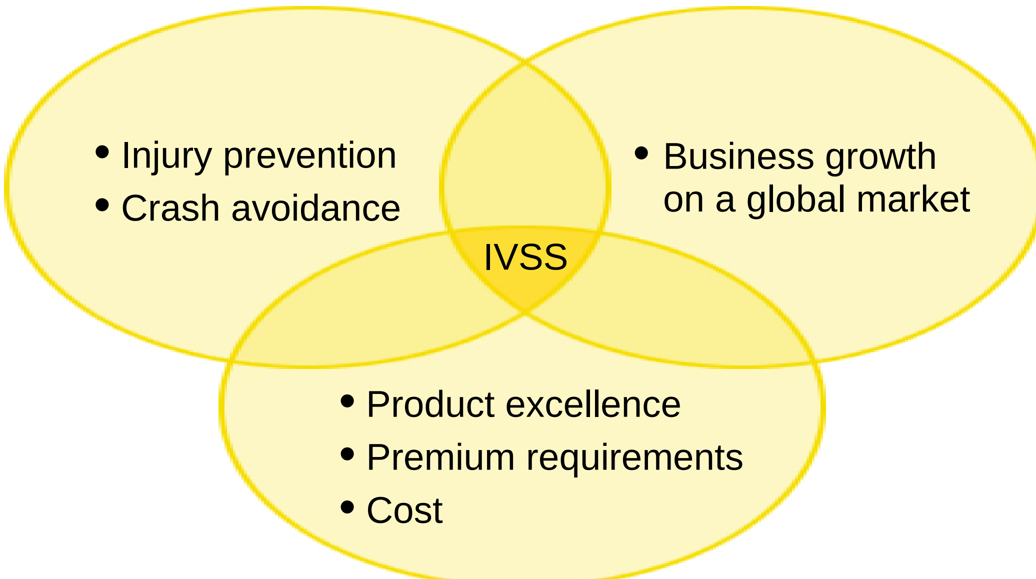

Three interacting components - for better safety, growth and competitiveness:

The human being

Preventive solutions based on the vehicle's most important component.

The road

Intelligent systems designed to increase security for all road users.

The vehicle

Active safety through pro-active technology.

Title of the report: A low-cost electrically steerable active antenna for adaptive cruise control and other applications

Authors: Herbert Zirath - Chalmers, Paul Hallbjörner, Jan Welinder - SP

Reference number: AL 80 A 2007:3356

Publication date: 2008-03-05

Contact person: Jan Welinder, jan.welinder@sp.se

Table of contents

1. Introduction

1.1 Automotive radar sensors

Sensors used by driver assistance systems have increasing importance in modern cars. They contribute to safety but also to cost and reliability. Cost effective and reliable sensor technology is therefore crucial for a successful introduction of active safety technology. Two frequency bands are used, 24 GHz and 77 GHz. The 2 GHz band is mainly used for short distance system with limited resolution. This band is temporary and will not be allowed to use for new systems from 2013. The 77 GHz band is currently used for long range system in automatic cruise control.

In this study a new technology for an automotive radar front was investigated aiming at lower cost. The performance of the sensor is suitable for long range radar. The study was financed by the Intelligent Vehicle Safety System programme, SP and Chalmers.

1.2 Current technologies

Currently several technologies are used for beam control in automotive radar sensors (see fig 1). The first units often had a movable antenna covering a sector in front of the vehicle. Mechanical steering is sensitive and difficult to make cheap. To avoid mechanics then beam switching was introduced. The signal is switched between several small transmitter antennas (in most cases 3-4). A beam is formed and focused with a dielectric lens. The different transmitter antennas will be focused in different directions and a large area covered by them together.

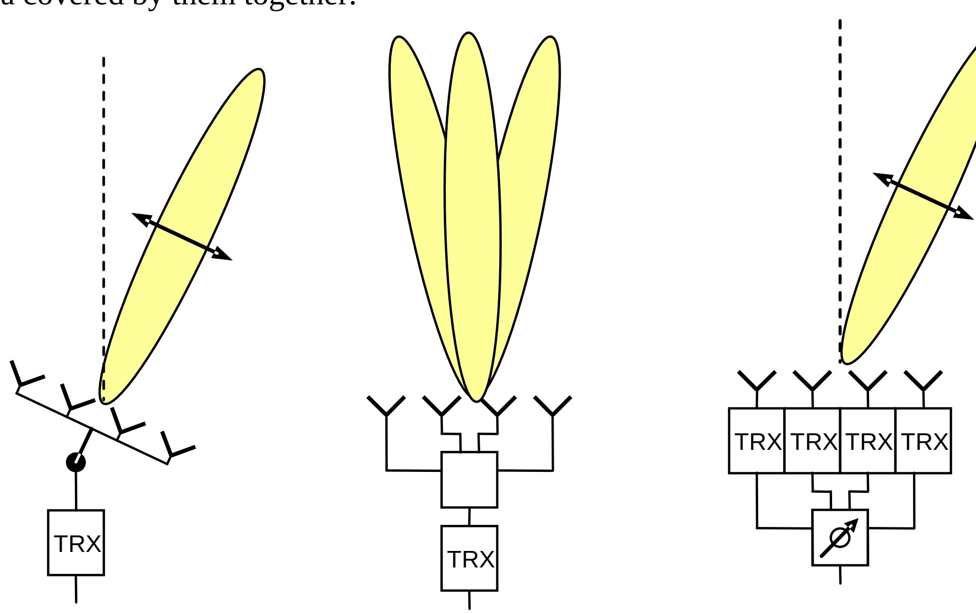

Fig 1. Radar front end technologies: mechanical steering, beam switching and digital beam forming.

The direction is found by comparing the echoes in several beams. If only a limited number of fixed beams are used they cannot be too narrow if a sufficient total angle shall be used. This reduces the resolution.
Digital beam forming is used in high end radar systems. A quite advanced signal processing electronics is feeding an antenna panel like in fig 3 (page 12). Each column pair is controlled by an individual power amplifier. This approach of course gives a wide range of possibilities. The most interesting is to control the phase for each antenna column and thus control the direction of the beam. However, the complicated construction will add to the cost and it is also likely that there will be problems to accurately control the many signal paths.

1.3 The low cost alternative

A much simpler approach has been investigated in this pre-study. It has many of the advantages of the digital beam forming but a much simpler construction. A simple analogue circuit is used instead of the complicated digital beam forming electronics. All antenna columns are fed by the same signal but between the pairs an analogue steerable phase shifter is placed. This is a cheap and simple component that will introduce a controlled phase delay between the columns that can be used for continuous beam steering.

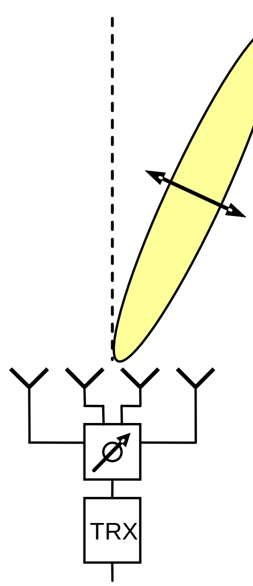

Fig 2. The phase shifter based front end.

The radar front end consists of the phase shifter together with the antenna. Signal processing adds important performance like the ability to separate several targets but can also contribute to finding the correct position of the target. The basic parameters like resolution and maximum distances are however mainly depending on the front end.

1.4 Results

Parameters in current systems are described in table 1 together with what was achieved in the pre-study. The study indicated that a higher resolution is a requirement

Parameter	**Current systems**	**Pre-study**
Range	150-200 m	150-200 m
Center frequency	79 GHz	79 GHz
Bandwidth		2 MHz
Antenna width		100 mm
Antenna height		50 mm
Antenna polarization	Vertical linear	Vertical linear
Horizontal 3 dB beam width	5°	2º
Vertical 3 dB beam width	10°	5º
Beam steering	Continuous	Continuous
Coverage	±6°	±5 º
Sidelobes		?
Antenna losses		9 dB

Table 1. Parameters of current systems compared with the performance of the proposed technology.

Link budget
The link budget is based on the antenna parameters that are studied in detail but also involves receiver circuitry parameters. The noise factor is estimated from similar circuits but the bandwidth is depending on the type of radar. The specified bandwidth of 2 MHz is large compared to the expected Doppler shift in the range of kHz. In a continued study it will probably be found that a narrower bandwidth might be used which would improve the link budget and increase the sensitivity of the radar sensor.

Range
The maximum range of current units is 150 – 200 m. There seems to be limited practical use of a much longer range. Systems with a much shorter range of e g 100 m are still useful in systems with limited but still important functions. At half the range the power of the received target signal increases 16 times which reduces the requirement for the electronics. A shorter range is possible to consider for cheap systems.

Resolution

The resolution of the sensor is mainly decided by its geometrical size. The highest resolution is required in the horizontal plane. Current systems often have a horizontal beam width of around 5°. This was the initial target for the study but high performance systems require a resolution of around 1° and thus a similar beam width. Improving the resolution to 1º will require a larger (200 mm) antenna panel. This will increase losses but also improve the gain and is probably achievable.

Coverage
A long range ACC system requires a horizontal scan of ±6° while a short range sensor for obstacle detection requires a much wider sector like ±50°. The coverage achieved in the pre-study was ±5° which is probably quite little. However, it can be improved by using more phase shifters. This will increase the losses and may affect the link budget.

1.4 Future work

That the technology is feasible has been shown in this study. To fully understand the possibilities and difficulties of the technology more work needs to be done.

A prototype needs to be built including a number of phase shifters placed on an antenna substrate where the actual antenna performance can be studied. It is crucial the all the phase shifters has the similar performance. Otherwise the beam wills spread and resolution is lost. The difference is expected to be small but it is for the moment not known.

The development towards a fully functional system can be made in several steps that are evaluated separately.

The applicability for short range systems has to be investigated. The main point of interest is if it is possible to sweep a much wider angle. This requires more phase shifters or a larger phase shift in each component.

2. Antenna

The antenna study aims at finding a cheap technology that still makes high performance feasible. Low substrate cost is critical together with cheap production technology. Other requirement are mechanical stability and electrical stability in severe climatic environments.

2.1 Link budget

The link budget is based on the well known radar equation:

$$\frac{P_r}{P_t} = \sigma \frac{G_t G_r \lambda^2}{(4\pi)^3 R^4}$$

The received power P_r shall exceed the noise power P_{noise} with at least 6 dB.

$$P_{noise} = kTBF$$

Typical system parameters are given in table 2.

Wave length	λ	0.0038 m
Distance	R	150 m
Target cross section Pedestrian	σ_{ped}	1 m^2
Target cross section motorcycle	σ_{mc}	5-10 m^2
Target cross section car	σ_{car}	30-100 m^2
Boltzmann´s constant	K	$1.3865 \cdot 10^{-23}$ J/K
Temperature	T	300 K
Bandwidth	B	2 MHz

Table 2: Given system parameters. The cross section is an equivalent cross section only loosely connected to the actual surface area.

Table 3 shows an example of a front end and its parameters. The directivity of 34 dBi corresponds to a beam width of 2º. This is less than the current for commercial units but gives and increased resolution in a high performance system. The losses are estimated from line losses of about 0.6 dB/cm and other antenna losses. These reduce the antenna gain to 29 dBi. A noise factor of 5 dB is assumed. The transmitter power is set somewhat arbitrarily to 1 dBm. The maximum legal power of 55 dBi would allow a transmitter power of 26 dBm. It is no possible to use that high power since it will be too expensive to generate. The heat dissipation will also be high and might complicate the radar module construction.

An additional problem is that the RF signal voltage will be high compared to the bias and the circuit is very non-linear. The suggested power level of 10 mW is quite easily achieved in current 77 GHz-generators but it will require some modification of the phase shifter to avoid non linear behavior.

Antenna size	A	0.1×0.05 m^2
Directivity	D	34 dBi
Total losses	L	9 dB
Antenna gain transmitter	G_t	25 dBi
Antenna gain receiver	G_r	25 dBi
Transmitter power	P_t	10 dBm
Noise factor	F	5 dB

Table 3: Examples of front-end parameters.

Using the parameters from table 2 and 3 we will get system performance according to table 4.

Target	**Distance**	**Received power**	**Noise margin**
Pedestrian	150 m	- 108 dBm	< 0
	100 m	-101 dBm	5 dB
Motorcycle	150 m	-101 dBm	5 dB
Car	150 m	-94 dBm	12 dB
	200 m	- 99 dBm	7 dB
Noise power		**-106 dBm**	

Table 4: Received power calculated from the values in table 2 and 3.The lower value for the radar cross section is used.

A noise margin of about 6 dB is normally required by the signal processing. This means that a car is easily detected at 150 m but a motor cycle is on the limit. It is probably not necessary to detect a pedestrian at the maximum distance.

The link budget can probably be improved. The band width of the receiver can very likely be reduced. If a smaller antenna panel is used the losses will decrease but the beam width will increase reducing the gain.

2.2 Panel

The phase shifter and the antenna in fig 3 gives performance as described in table 4. The phase shifter will generate a maximum phase shift of 23 - 55° according to the simulations depending on the configuration. Using 15 columns the total shift is 345 – 825°. For a 100 mm wide panel this will generate a beam shift of 2 – 5º. If the feed direction is changed the total scan width is doubled to 4 - 10º.

The panel used in the calculations is shown in fig 3.

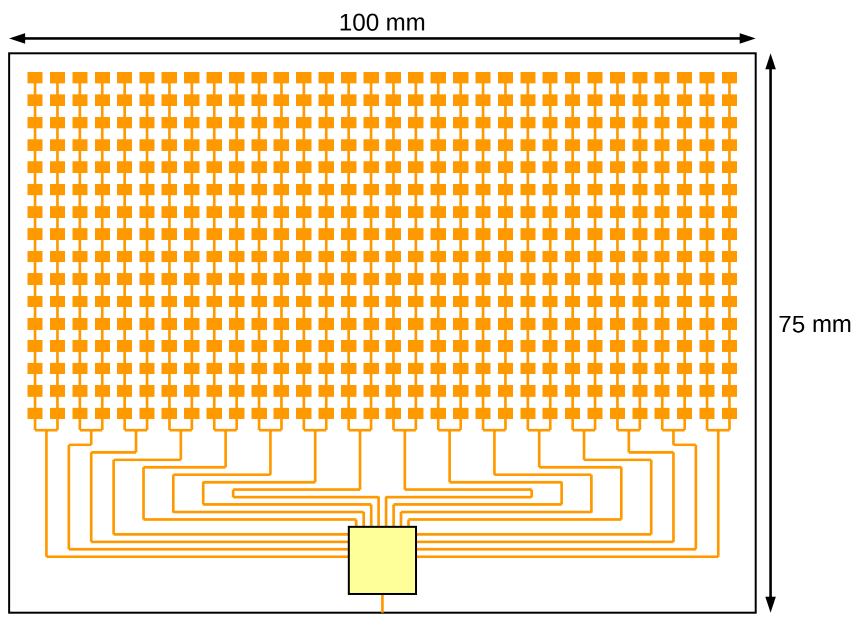

Fig 3. Front end used in the calculation.

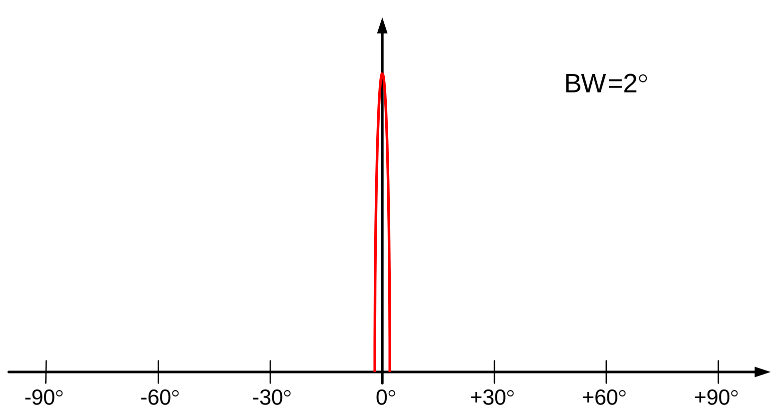

Fig 4. Antenna beam.

The technology can be used for other configurations as shown in fig 5 and 6.

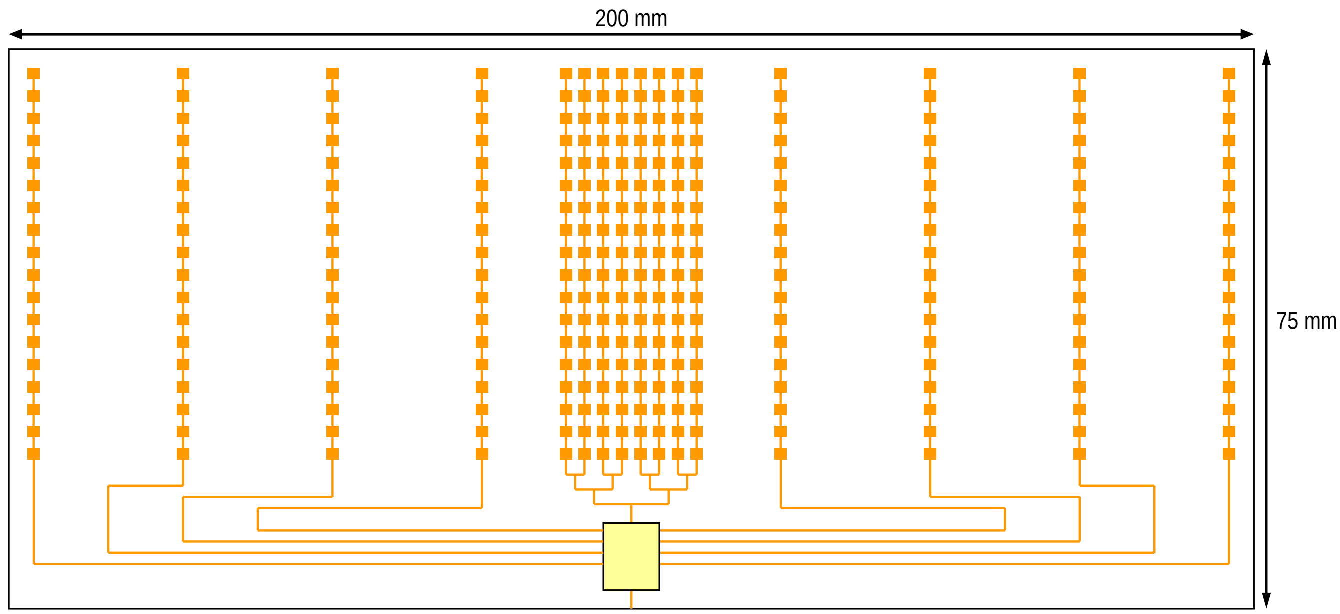

Fig 5 Alternative front end with an antenna with a wide beam combined with a sparse grid that generates several very narrow beams (see fig 4).

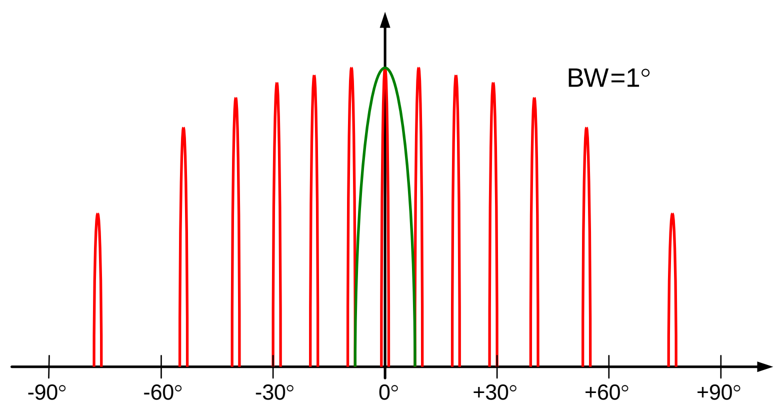

Fig 6. Antenna pattern for the combined antenna in fig 5. Signal processing has to be used combining the two antennas to obtain the full resolution.

2.3 Substrate

The requirements for the substrate are estimated from previous studies and experiences in the 60 GHz range. These are partly from industrial projects and not published. A comparison with commercially available polymer materials shows that cheap materials may be used. There are also unpublished experiments supporting this.

	Value	**Tolerance**	**Taconic TaclamPlus[1]**	**Rogers RT/duroid 5870[2]**
Permittivity ε_r		<±0.02	2.17±0.02	2.33±0.02
Dielectric losses $\tan\delta$			0.0008[3]	0.0012[3]
Dielectric thickness	50-150 μm	<±10 %	100±10 μm[4]	127±13 μm
Moisture absorption		<0.02 %	0.02 %	0.015 %
Etch accuracy		<2 μm		
Cu thickness	<10 μm		9 μm	9 μm
Planarity		<±0.05 mm		
50 Ω line width			0.31 mm	0.38 mm
1 λ line length			2.7 mm	2.6 mm

Table 1: Substrate tolerances and parameters with accuracy of two commercially available substrates.
[1]Alternatively TLP or TLY.
[2]Alternatively RO4350B or RO3003.
[3]Not at the frequency in question.
[4]Accuracy esitmated from photograph of cross section.

Cost depends strongly on volume, but roughly SEK 10 per substrate. It is not clear how much of this is the substrate material cost and how much is the processing cost.

2.4 Scan angle

The maximum phase shift in the various simulated configurations is 23 – 55º. Using 15 phase shifters the total phase shift will be 420º – 825º. The phase shifter might be fed from both directions thus doubling the total phase shift to 820º – 1650º.

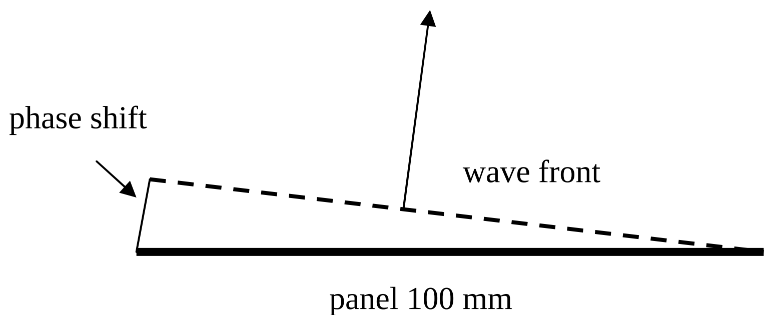

Fig 7. The total phase shift over the panel will tilt the wave front.

Using a wave length of 3.8 mm will give a total scan angle of up to 10º. This is slightly less than current constructions.

3. Phase shifter

The aim of this study is to investigate the feasibility of using commercial semiconductor technology in order to realize phase shifters for future ‘small sized’ radar systems that use continuos electronic scanning. Initial system studies indicate specification goals of 40-50 degrees of electronically controlled phase shift with an insertion loss less than 0.5 dB. A phase-shifter of type ‘transmission line phase shifter’ was chosen. Some realizations of such phase shifters using ideal components are shown in Fig 1-3. Simulations of two-load TTPS phase shifters were done using commercial software ADS from Agilent.

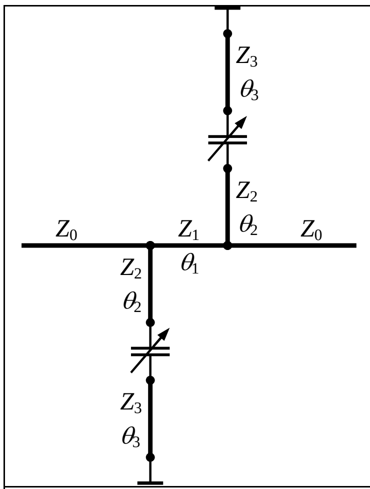

Fig. 1 Two-load TTPS (phase shift = 32°, delay = 200°) TTPS with shorted stubs

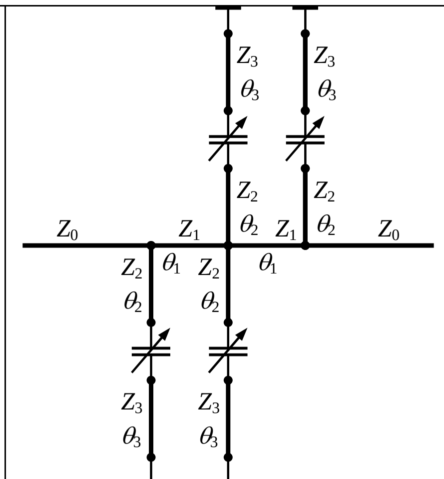

Fig. 2 Four-load TTPS (phase shift = 64°, delay = 400°) TTPS with shorted stubs

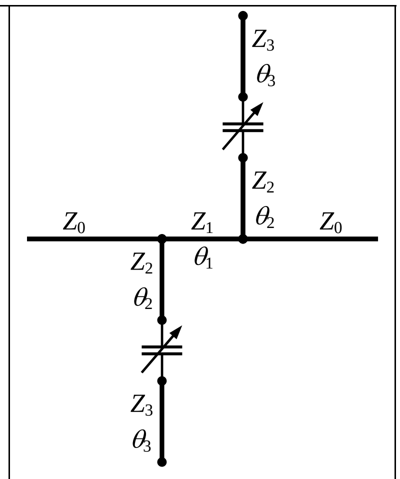

Fig.3 Two-load TTPS with open stubs (phase shift = 40°, delay = 150°)

	Variant 1	Variant 2	Variant 3
Z_1	80 Ω	100 Ω	110 Ω
θ_1	37°	29°	25°
Z_2	50 Ω	50 Ω	50 Ω
θ_2	10 °	10 °	10 °
Z_3	50 Ω	50 Ω	50 Ω
θ_3	140°	145°	150°

TABLE 1 TTPS with shorted stubs

Z_1	110 Ω
θ_1	26°
Z_2	50 Ω
θ_2	11 °
Z_3	50 Ω
θ_3	55°

TABLE 2 TTPS with open stubs

3.1 Simulation of two and four load phase shifters using idealized components

3.1.1 two-load TTPS, three variants

The ADS-simulation setup page for the two-load TTPS with shorted stubs (variant 1) is shown in Fig. 4. The capacitances are swept in the simulation, from 20 to 80 fF. The series and parallel resistances of the varactors are assumed to be of the order 1 ohm and 500 ohm respectively. These values are typical but have to be determined more accurately in future designs, the purpose at this moment is to understand the influence of these parasitic components which are related to the losses in the varactor.

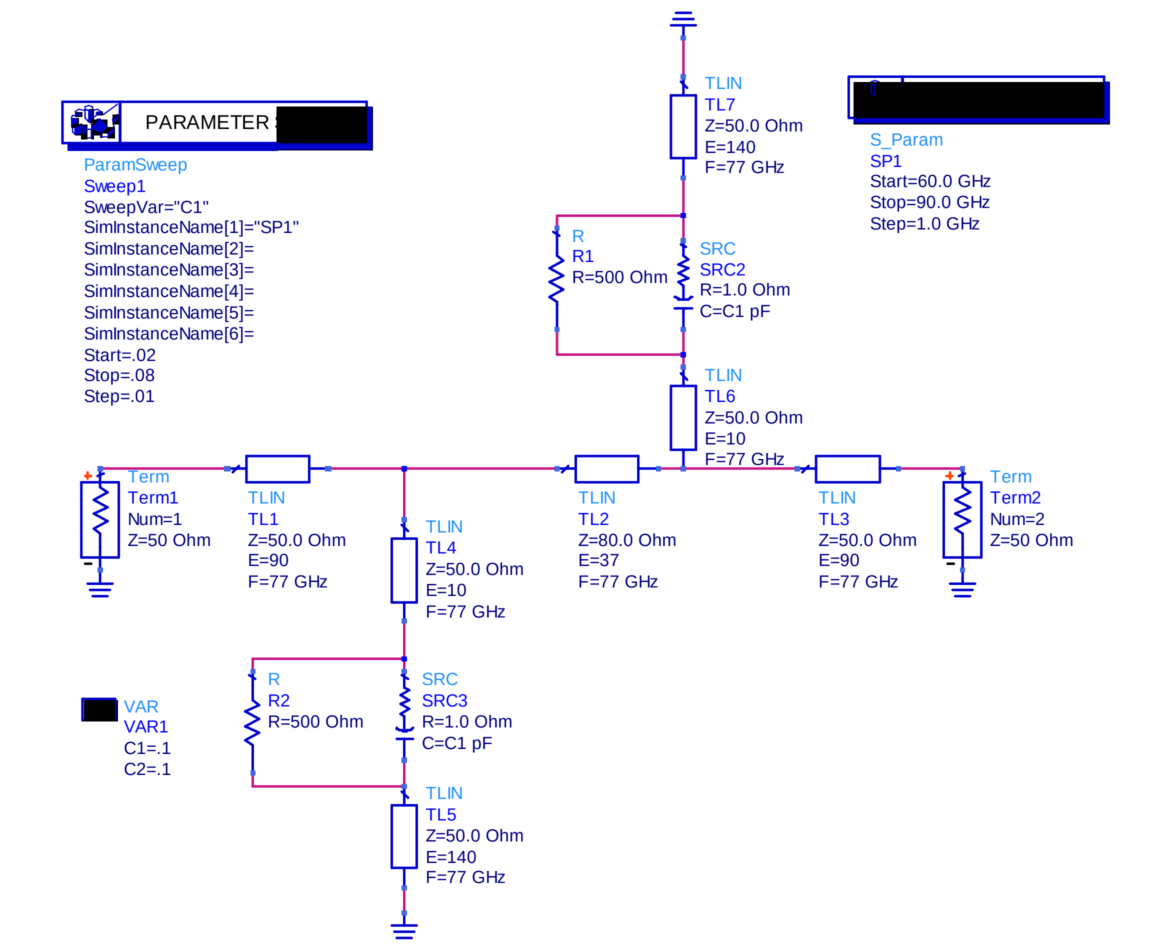

Fig. 4 ADS Circuit and simulation page for TTPS with shorted stubs (variant 1)

The result of the simulation is shown in Fig. 5. The frequency is swept from 60 to 90 GHz with 1 GHz steps. Markers m4 and m5 for 77 GHz give max and min phase 105 and 77.6 degrees. The insertion loss is typically less than 0.5 dB at 77 GHz.

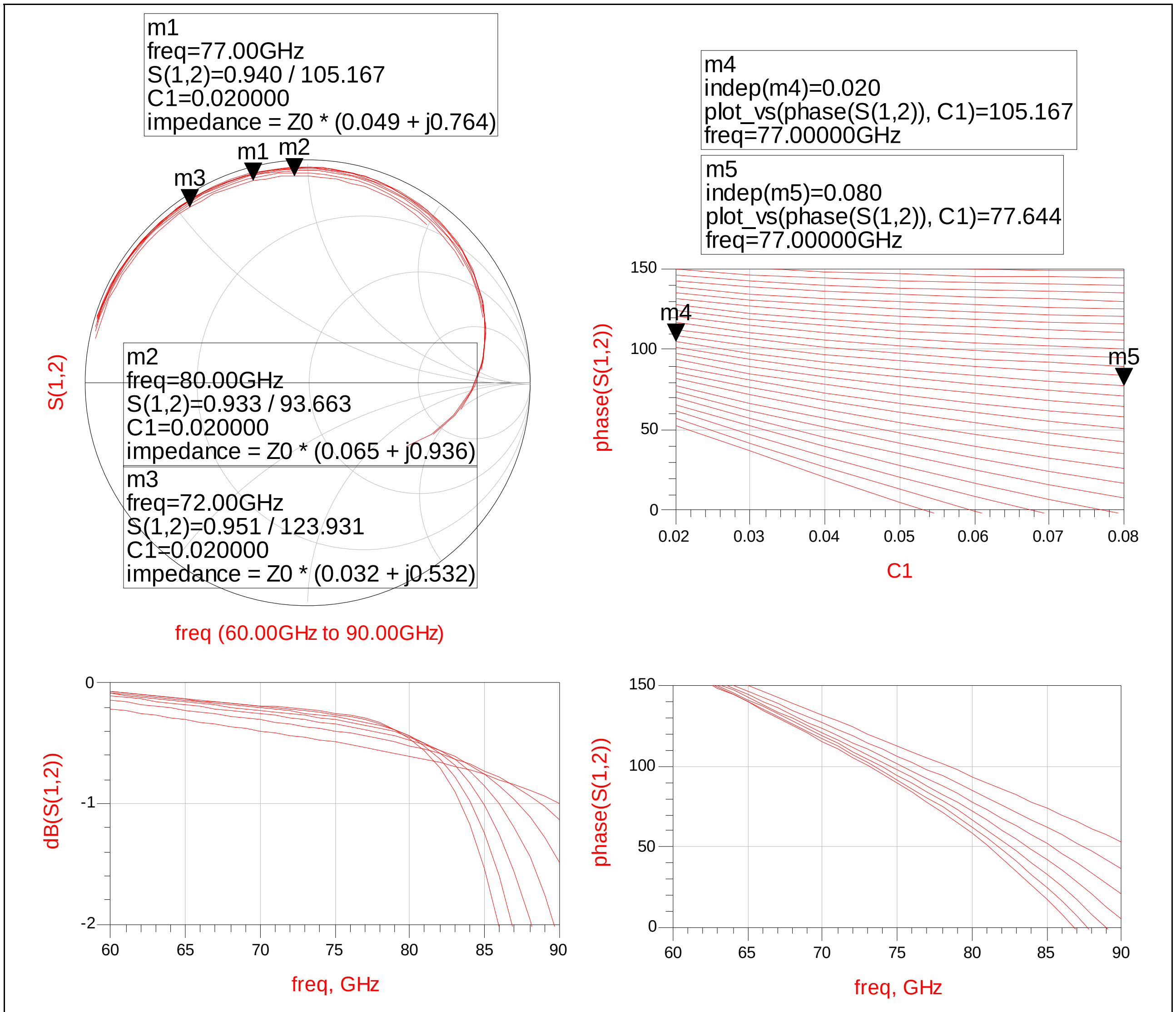

Fig. 5 Simulation results for TTPS with shorted stubs (variant 1)

The ADS-simulation setup page for the two-load TTPS with shorted stubs (variant 2) is shown in Fig. 6. The capacitances are swept in the simulation, from 20 to 80 fF. The series and parallel resistances of the varactors are assumed to be of the order 1 ohm and 500 ohm respectively.

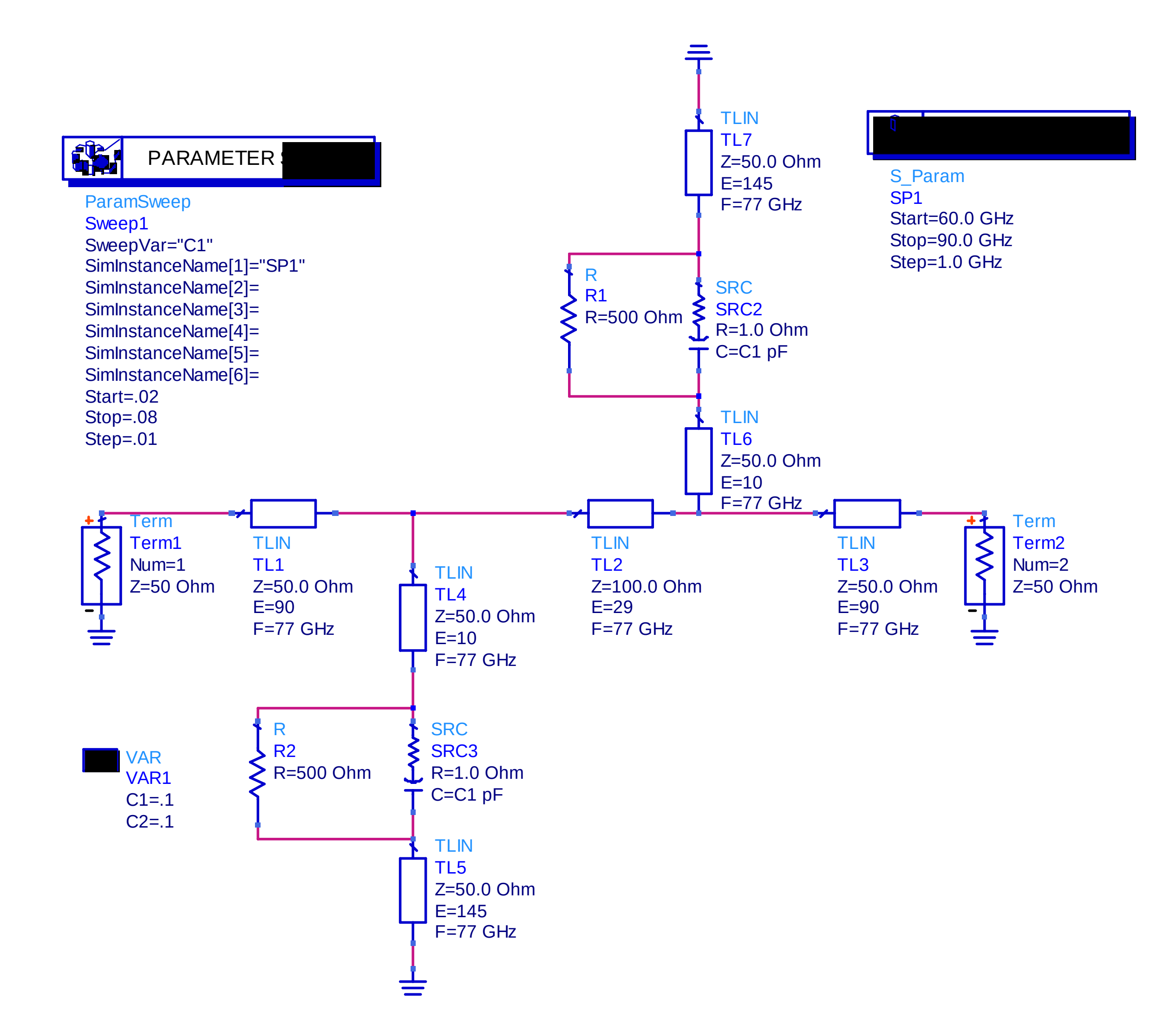

Fig. 6 ADS Circuit and simulation page for TTPS with shorted stubs (variant 2)

The result of the simulation of variant 2 is shown in Fig. 7. The frequency is swept from 60 to 90 GHz with 1 GHz steps. Markers m4 and m5 for 77 GHz give max and min phase 108.3 and 75 degrees i e a phase difference of 33 deg. The insertion loss is typically less than 0.5 dB at 77 GHz.

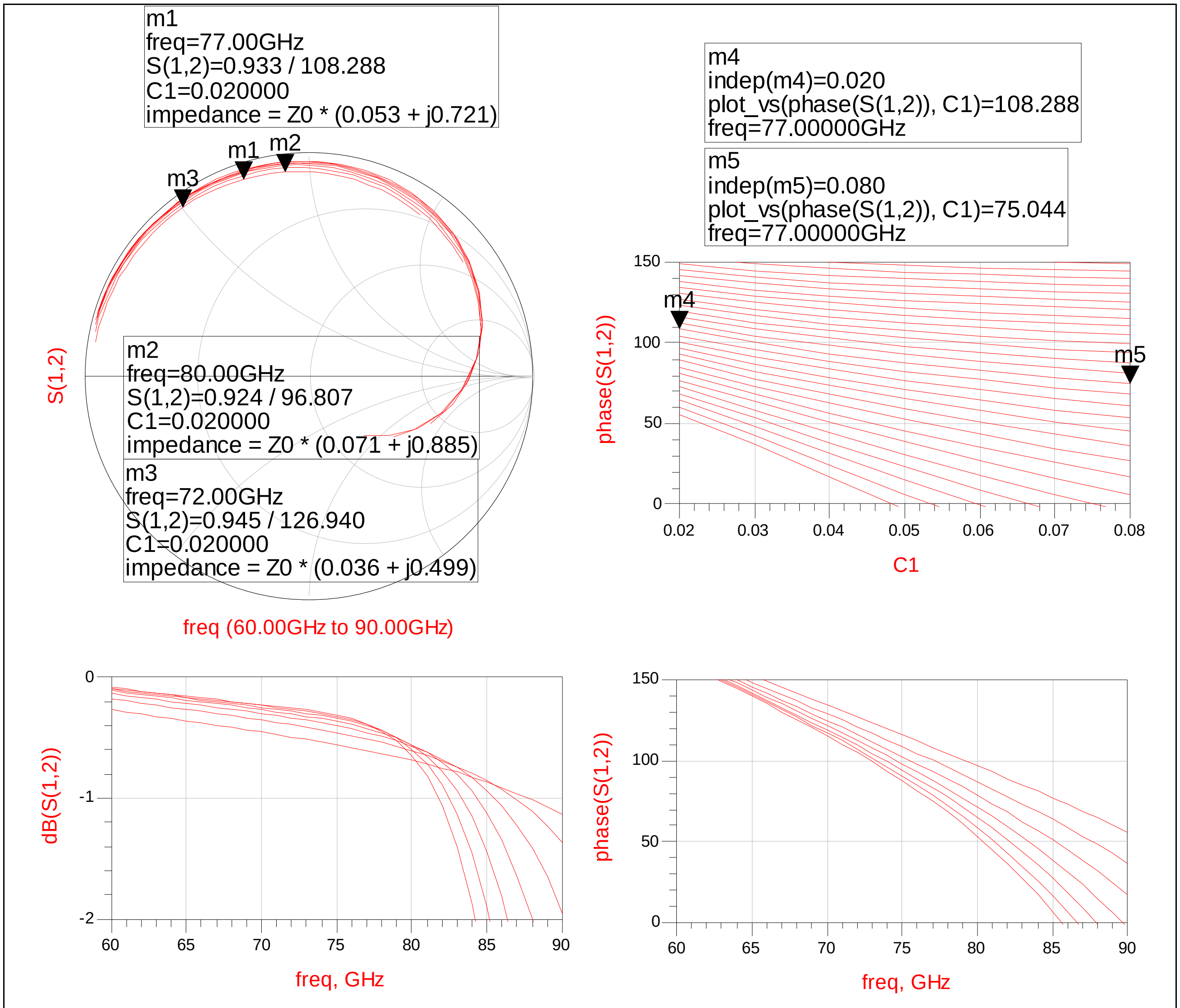

Fig. 7 Simulation results for TTPS with shorted stubs (variant 2)

The ADS-simulation setup page for the two-load TTPS with shorted stubs (variant 3) is shown in Fig. 8. The capacitances are swept in the simulation, from 20 to 80 fF. The series and parallel resistances of the varactors are assumed to be of the order 1 ohm and 500 ohm respectively.

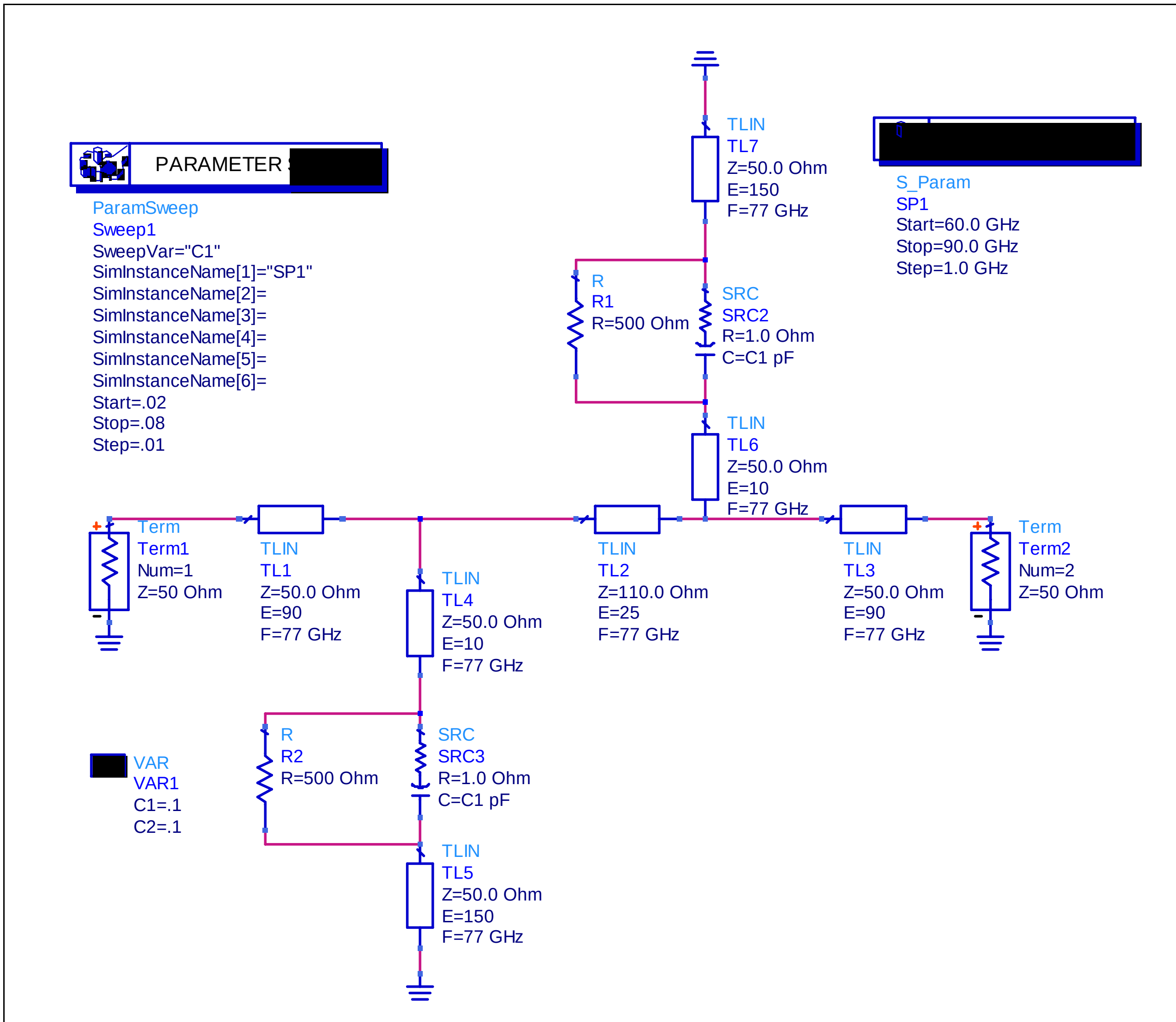

Fig. 8 ADS Circuit and simulation page for TTPS with shorted stubs (variant 3)

The result of the simulation of variant 3 is shown in Fig. 9. The frequency is swept from 60 to 90 GHz with 1 GHz steps. Markers m4 and m5 for 77 GHz give max and min phase 110.5 and 72.3 degree i e a phase difference of 38 deg. The insertion loss is typically less than 0.5 dB at 77 GHz.

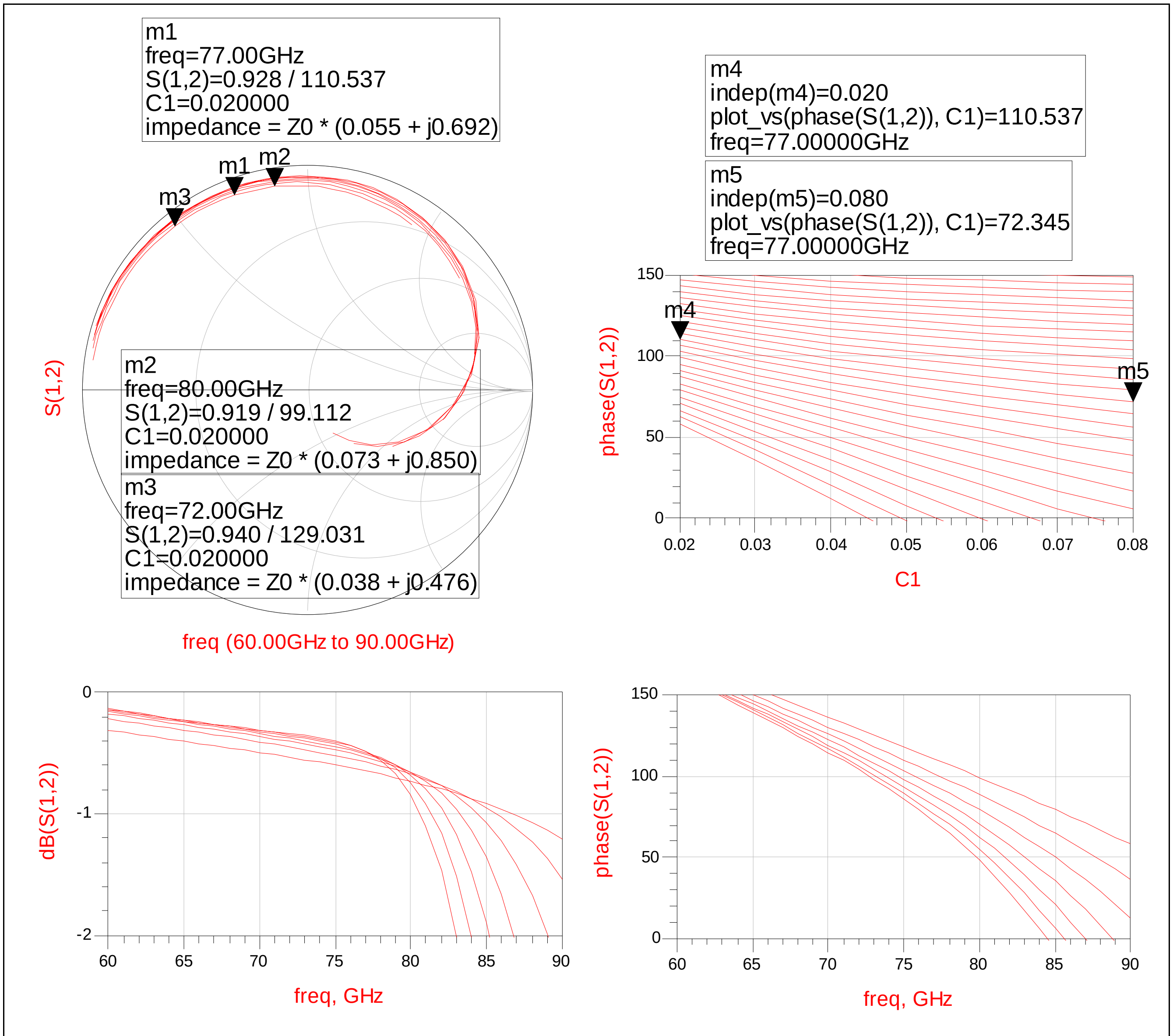

Fig. 9 Simulation results for TTPS with shorted stubs (variant 3)

3.1.2 four-load TTPS

The ADS-simulation setup page for the four-load TTPS with shorted stubs is shown in Fig. 10. The capacitances are swept in the simulation, from 20 to 80 fF. The series and parallel resistances of the varactors are assumed to be of the order 1 ohm and 500/1000 ohm respectively.

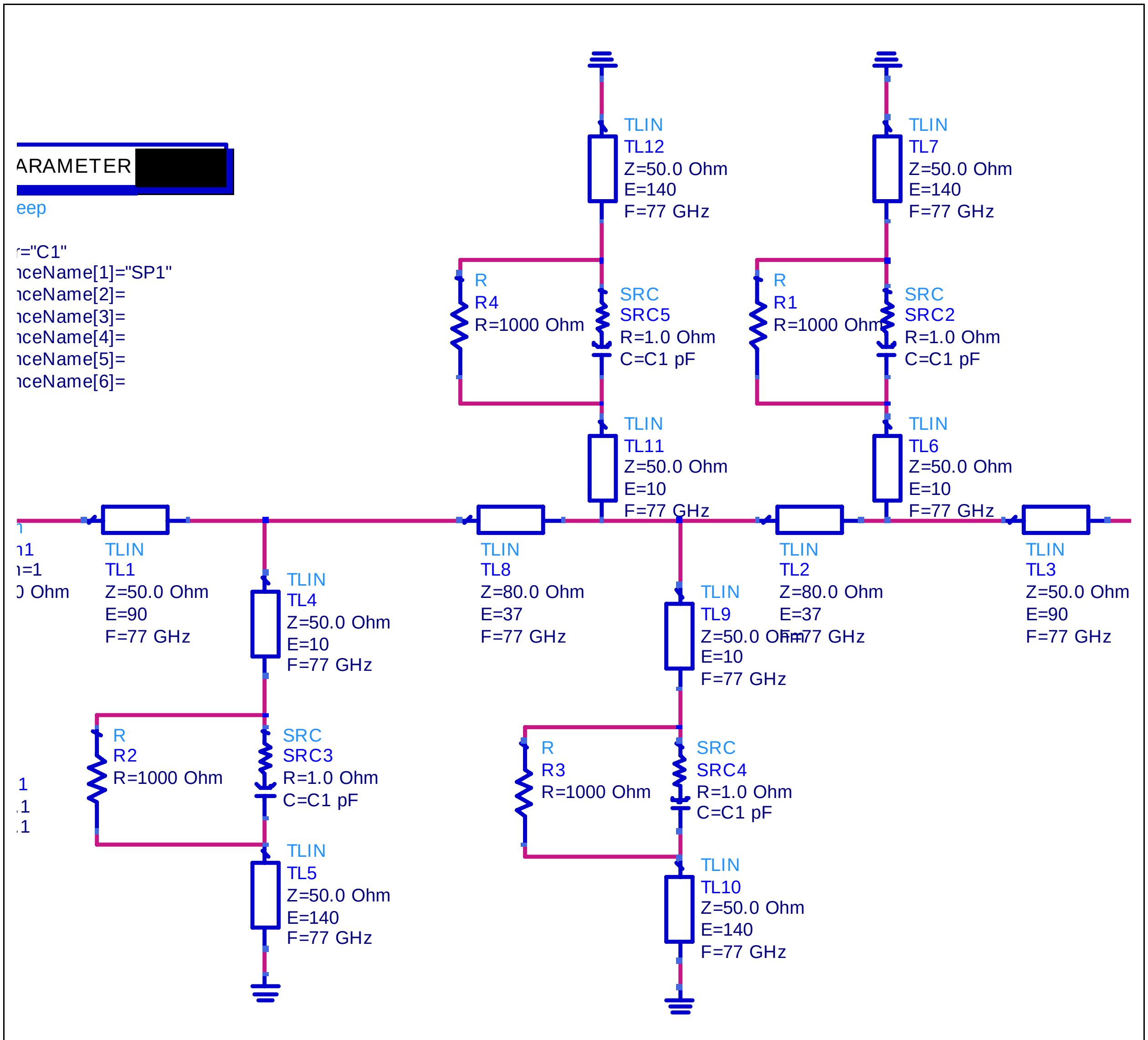

Fig. 10 ADS Circuit and simulation page for a four-load TTPS with shorted stubs (Rp=500 ohm)

The result of the simulation of the four-load TTPS is shown in Fig. 11. The frequency is swept from 60 to 90 GHz with 1 GHz steps. Markers m4 and m5 for 77 GH gives max and min phase -2.6. and 30.6 degree i e a phase difference of 55.2 deg. The insertion loss is typically less than 0.5 dB at 77 GHz.

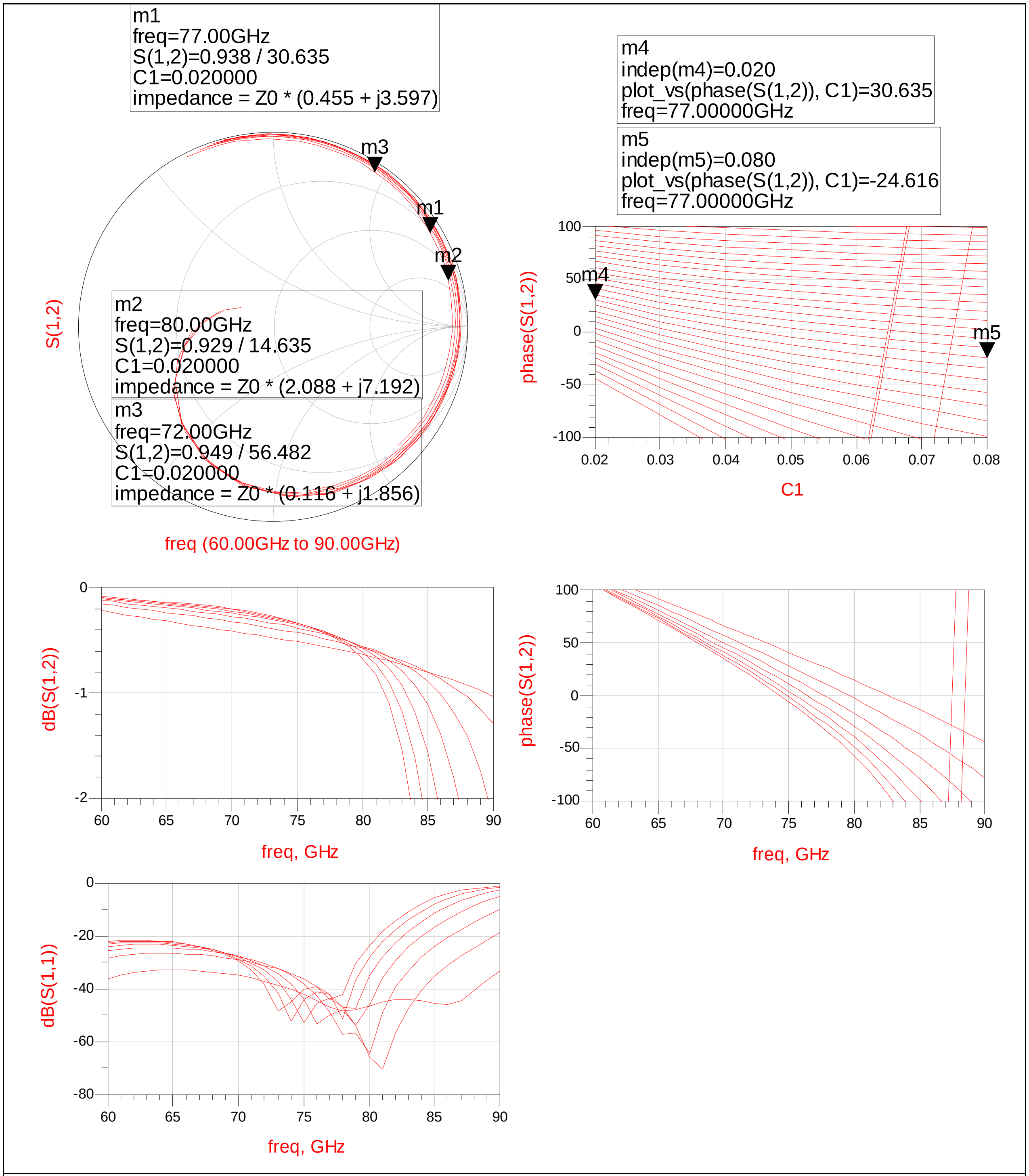

Fig. 11 Simulation results for a four-load TTPS with shorted stubs (variant 3) Rp=500

3.2 Technology choice

Several semiconductor technologies are good candidates for the realization of the phase shifters. For the realization of system demonstrators, GaAs pHEMT and mHEMT technologies are possible as well as bipolar technologies like InGaP-GaAs HBT and InP based HBT processes. For very high manufacturing volumes (>10 Milj) silicon technologies such as SiGe HBT and deep submicron CMOS are interesting alternatives. Due to the availability of mHEMT MMIC processes at MEL/Chalmers, we have chosen an mHEMT technology for this feasibility study. The main critical parameters are

1. Varactor losses
2. Capacitance variations of the varactor, Cmin/Cmax
3. Losses in transmission lines, transitions etc

Varactor characteristics for the MP15 0.15 µm gatelength mHEMT technology from WIN Semiconductor

In an integrated circuit technology, varactors are usually not a standard component. Varactor diodes can be realized by using either p-n junctions (if bipolar transistors are available in the process), or Schottky junctions. In some processes, these varactors are available as a modeled layout component in the designkit, however not necessarily optimized for high Q-value. This might then be the task of the circuit designer if high Q varactors are important. The varactor characteristic, i e S11, for the Schottky varactor diode in the MP15-process, based on our in-house transistor nonlinear model, is shown in Fig. 12.

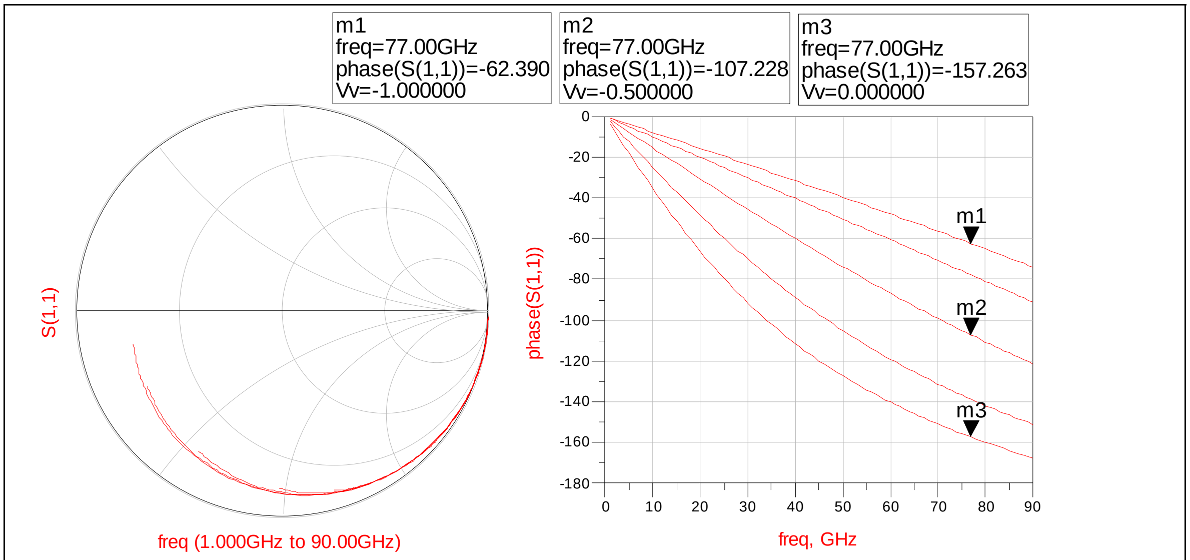

Fig. 12 Reflection coefficient for a Schottky diode (with anode shorted) as a function of cathode bias voltage. The bias voltage is swept from 0 to -1V in 0.25 V steps. The frequency is swept from 1 to 90 GHz.

The transistor size is 2·25 µm which is used in the phase shifter MMIC realized in this project. The source and the drain of the transistor are tied together forming a diode. Calculation of the capacitance, reflection coefficient, Q-value, and series resistance, as a function of the cathode bias voltage, Vcb, is performed by using the formulas shown in Fig. 13. It is assumed that the diode is described as a capacitor and a series resistance, which seem to be a good approximation after inspection of frequency dependence of the reflection coefficient, Fig. 12. From Fig. 13 we can conclude that the capacitance can be changed from 25 to 200 fF, the series resistance is quite constant between 6-7.2 ohm, the Q-value is varying from 13 to 1.5, as the bias is changed from 0 to 1 V. The model (so called Chalmers model) is based on multibias S-parameter measurements on a transistor with emphasis on *transistor operation*. This model is at the moment 'best effort' and is used in the design of the first phase shifter for this feasibility study. The model is not at all developed for this application but is anyway sufficiently accurate to serve the purpose. From these simulations, we can conclude that a varactor based on a transistor with size 2.25 µm is a proper choice for a phase shifter in terms of capacitance range; the series resistance is sufficiently low for proper operation but is a candidate for optimization in future designs. It is however also important to make varactor measurements at 77 GHz to confirm the model in the future.

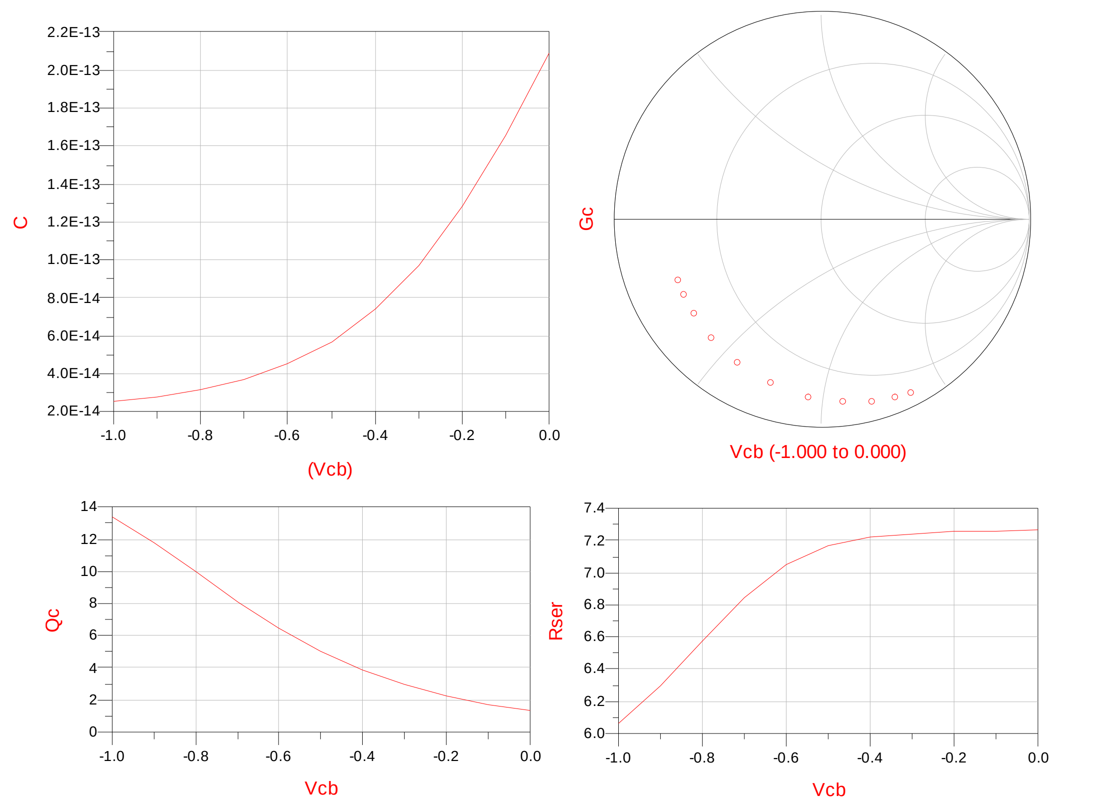

Fig. 13 Calculation of the capacitance, reflection coefficient, Q-value, and series resistance, as a function of the cathode bias voltage, Vcb. Model equations are shown to the right.

Rser=real(Zc)
Zc=vc[::,1]/ic.i[::,1]
Qc=-imag(Zc)/real(Zc)
C=-1/(2*pi*measfreq*1E9*imag(Zc))
Gc=(Zc-50)/(Zc+50)

3.3 Design of a two load phase shifter utilizing the commercial mHEMT process MP-15 (WIN)

A two load phase shifter based on the TTPS, variant 3, described in Fig. 8 was designed based on our ‘first approximation’ varactor model previously described for the commercial process MP-15 from WIN semiconductor, and our ‘in-house’ design kit. The designed phase-shifter can be regarded as a ‘model phase shifter’ serving the purpose to demonstrate the feasibility of the MP-15 technology, the models, the design kit components, and hopefully give some input to the system simulation as well as measurement methods. The phases-shifter was simulated in ADS utilizing em-modeled passive transmission line components (developed ‘in-house’) and the layout was generated. A special varactor layout was developed in order to minimize parasitic capacitances, the biasing of the varactors is through the bias-tee of the network analyzer’ test-set in order to simplify the characterization and modeling of the circuit. In a next-generation design, the bias-circuits can of course be integrated too, by adding an inductor and blocking capacitors. The simulation page and circuit description are shown in Fig. 14. Fig. 15 shows the layout generated by ADS, and Fig. 16 shows a photo of the fabricated circuit. The input and output of the phase shifter is accessed through CPW-pads. The simulation of the phase-shifter is shown in Fig. 17. The bias is 0, 0.5, and 1V. Note that then phase is plotted within -/+ 180 degrees in ADS. Characteristic resonances in S21 occur at 28, 37 and 44 GHz for 0, 0.5, and 1 V respectively, where the stubs are ‘quarter wavelength’. Since the operation at 77 GHz is of special interest, a plot from 65-85 GHz is shown in Fig. 18 for the same bias points but with 0.25 V steps. According to simulations, the phase difference is 23 degrees when the bias is swept between 0 and 1 V at 77 GHz. The loss is varying between 0.35 (1V) to 1.16 dB (0V). At 65 GHz, the frequency difference is 6 degrees and the loss is varying between 0.22 to 0.35 dB.

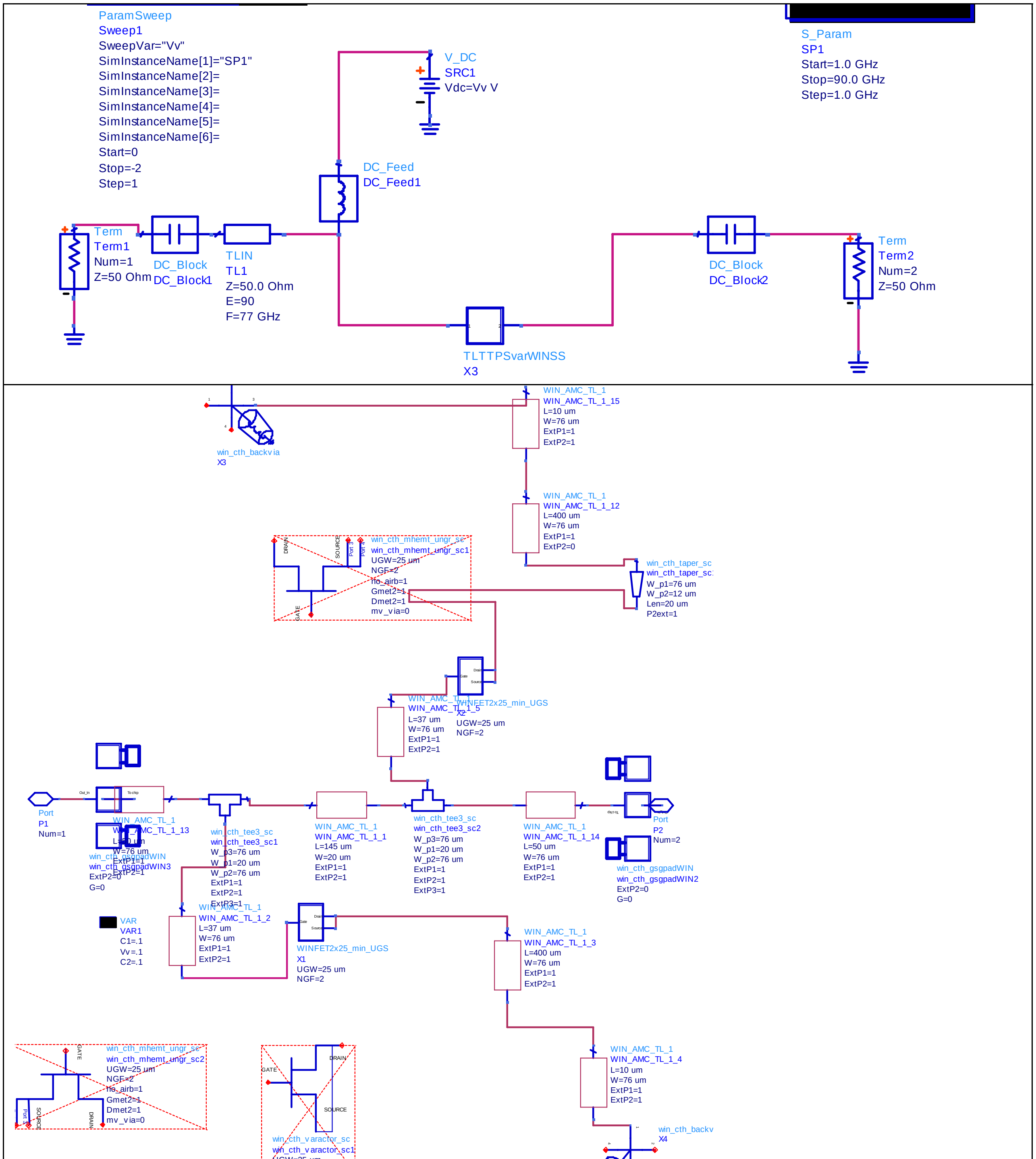

Fig. 14 The simulation page and circuit representation of the phase shifter

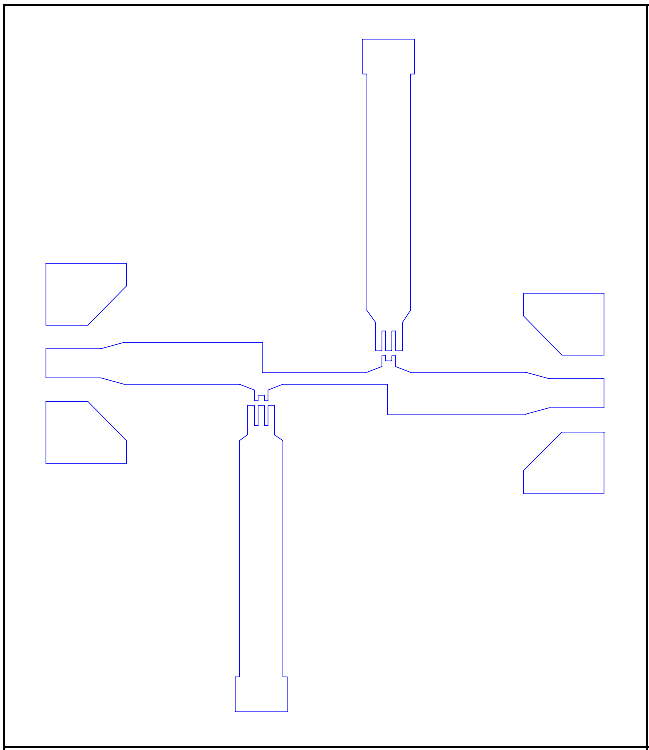

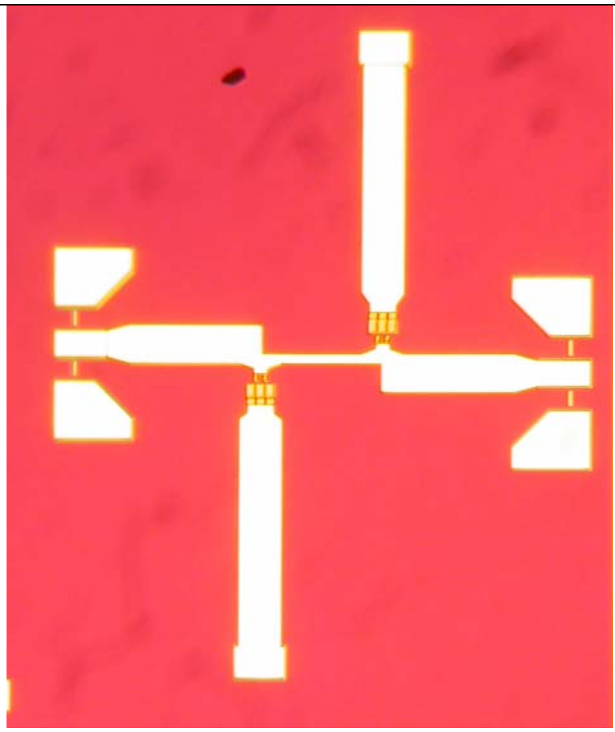

Fig. 15 Layout of phase-shifter	Fig. 16 Photo of phase-shifter. The circuit area is 1 mm^2.

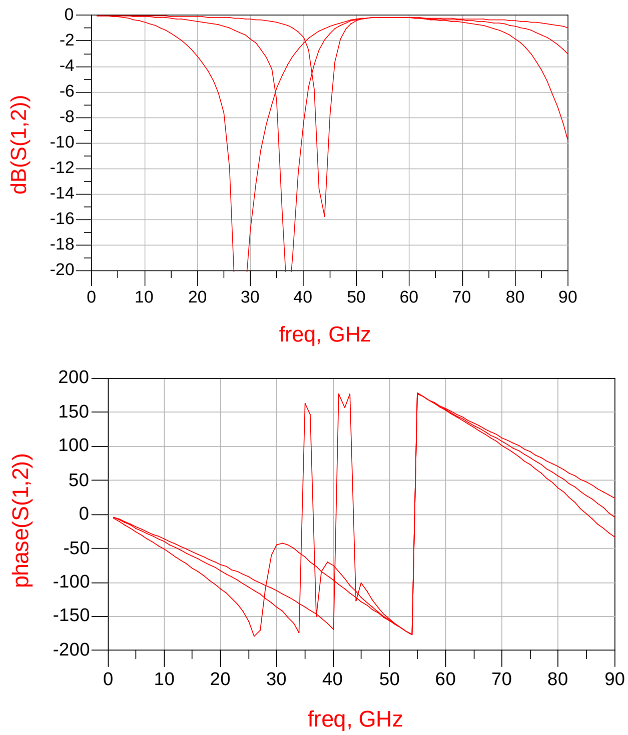

Fig. 17 Simulation results of the phase shifter, the frequency is swept from 1 to 90 GHz. The varactor bias is 0, 0.5 and -1 V.

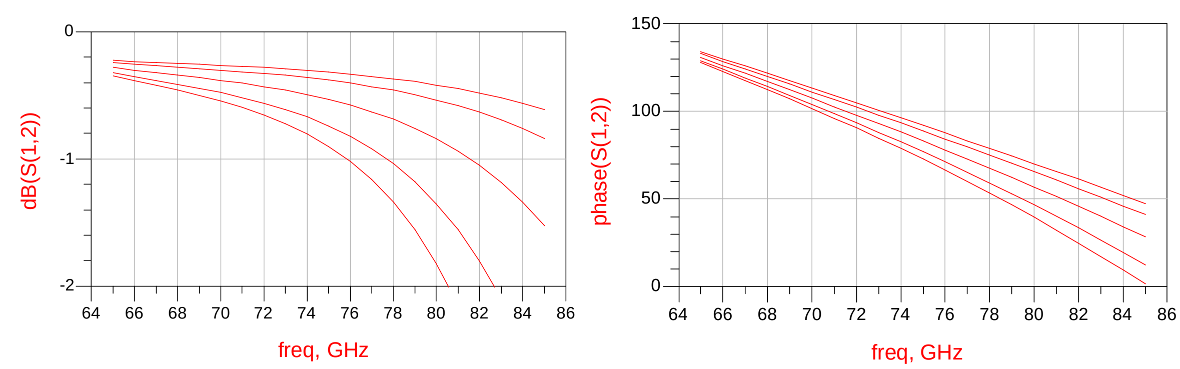

Fig. 18 Simulation results of the phase shifter, the frequency s swept from 65 to 85 GHz. The varactor bias is varied from 0 to 1 V, with 0.25 V steps.

3.4 Measurement results for the fabricated MMIC phase shifter

Measurement of the fabricated MMIC phase shifter was performed from 1 GHz up to 67 GHz. Measurements in W-band 75-115 GHz is possible at MEL but the VNA is not operational at the moment, and the measurements in this band have to be postponed until the beginning of 2008. Some conclusions can be made anyway from the 1-67 GHz measurements. S21 magnitude and phase is plotted in Fig. 19-21. From Fig. 19 we can conclude that the resonances seen from simulations also occur in the measurements, ranging from 32 to 38 GHz. The losses at 67 GHz is of the order 0.26-0.31 dB in good agreement with simulations. The phase shift is 7 degrees (for Vvar=0 to 1V) which is the same as the simulated value.

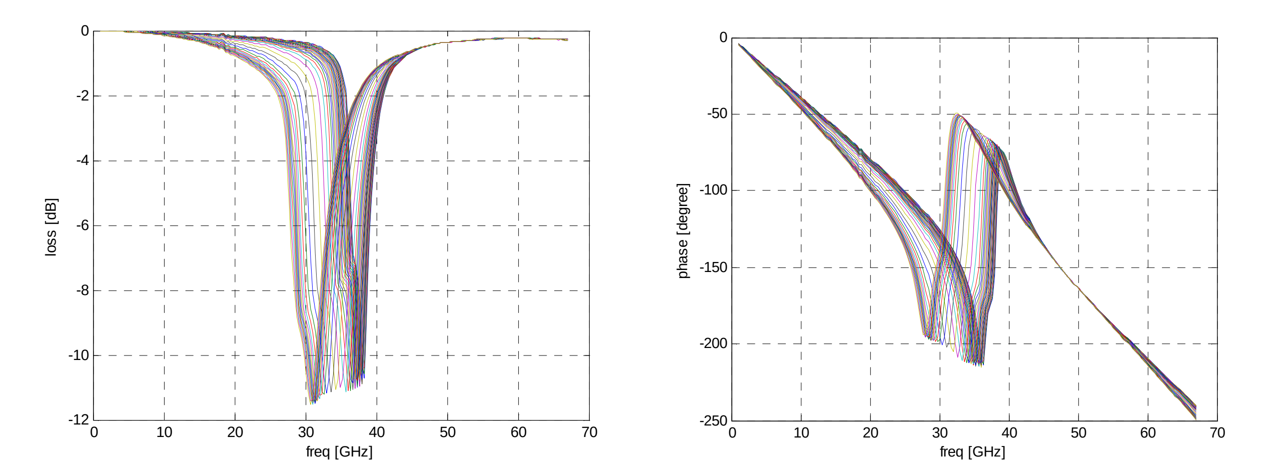

Fig. 19-20 Measured loss and phase versus frequency

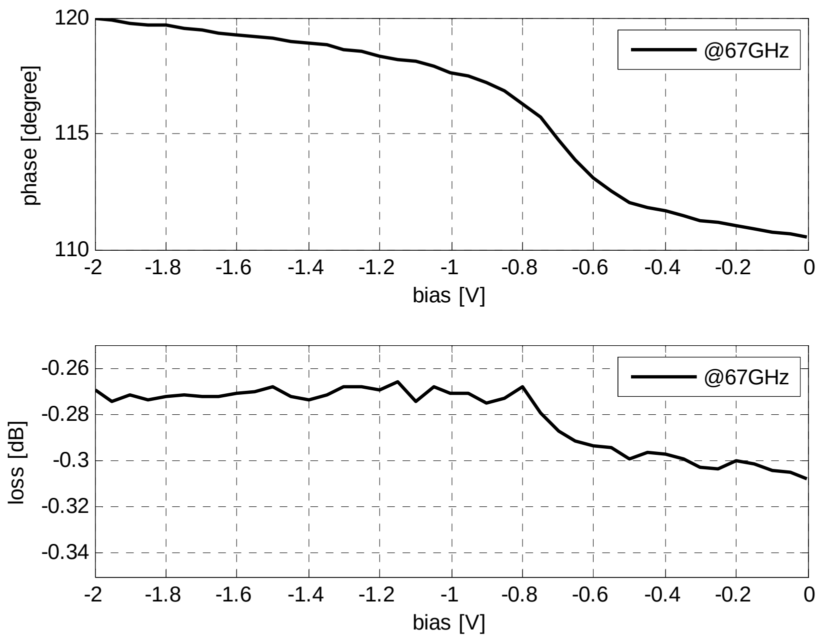

Fig. 21 Measured loss and phase at 67 GHz versus bias

3.5 Cost estimation of the phase-shifter

The cost of the phase shifter is dependent on the quantity, in large volume, the cost of a full 6" wafer is targeted to 2-3000 $ in the near future. The circuit area of the fabricated phase-shifter is of the order 1 mm^2. The estimated cost per phase-shifter is SEK 1.10 in very large quantity. In development phase the cost of a wafer is of the order 140k$.

3.6 Summary

Different transmission line phase shifters have been analyzed and one phase-shifter was designed, fabricated, and measured utilizing a commercial mHEMT process from WIN semiconductor. Although the measurement is not fully completed, the results are very promising. Most likely, phase shifters for this application can be realized in the proposed mHEMT technology with sufficient performance.

IVSS partners:

Intelligent Vehicle Safety Systems

Postal address: IVSS/Swedish Road Administration, SE–781 87 Borlänge, Sweden
Street address: IVSS/Swedish Road Administration, NAVET, Lindholmspiren 5, Gothenburg, Sweden
Phone: +46 (0)771 119 119
ivss@vv.se
www.ivss.se